Assessment of rock glaciers and their water storage in Guokalariju, Tibetan Plateau

Mengzhen Li, Yanmin Yang, Zhaoyu Peng, Gengnian Liu

College of Urban and Environmental Sciences, Peking University, Beijing, 100871, China

5 *Correspondence to*: Gengnian Liu (liugn@pku.edu.cn)

Abstract. Rock glaciers are important hydrological reserves in arid and semi-arid regions. Rock glaciers' activity states can indicate the existence of permafrost. To help explore further the development mechanisms of rock glaciers in semi-arid and humid transition regions, this paper provides a detailed rock glacier inventory of the Guokalariju (GKLRJ) area of the Tibetan Plateau (TP) using a manual visual interpretation of Google Earth

10 Pro remote sensing imagery. We also estimated the water volume equivalent (WVEQ) in the GKLRJ for the first time. Approximately 5,057 rock glaciers were identified, covering a total area of ~404.69 km². Rock glaciers are unevenly distributed within the three sub-regions R1, R2 and R3 from east to west, with 80% of them concentrated in R2, where climatic and topographic conditions are most favorable. Under the same ground temperature conditions, increases in precipitation are conducive to rock glaciers forming at lower altitudes.

15 Indeed, the lower limit of rock glaciers' mean altitude decreased eastward, with increasing precipitation. Estimates of the water storage capacity of rock glaciers obtained by applying different methods varied considerably, but all showed the potential hydrological value of rock glaciers. The maximum possible water storage in the subsurface ice of rock glacier permafrost was 3.04 km³, which is about 33% of the surface ice in local glacier storage. In R1, where the climate is the driest, the water storage capacity of rock glaciers was

20 estimated to be up to twice as large as that of the sub-region's glaciers. Changes in water resources and permafrost stability in the area where rock glaciers distributed will have implications for regional water resource management, disaster prevention, and sustainable development strategies.

1 Introduction

Rock glaciers are periglacial landforms often observed above the timberline in alpine mountains. They are

25 formed by rocks and ice that move down a slope, driven by gravity (French, 2007; RGIK, 2022a). As striking features of viscous flow in perennially frozen materials, they can reflect permafrost conditions in mountainous areas. Their lowest altitudes are often considered to represent the lower limit of discontinuous regional permafrost occurrence (Giardino and Vitek, 1988; Barsch, 1992, 1996; Kääb *et al.*, 1997; Schmid *et al.*, 2015; Selley *et al.*, 2018; Baral *et al.*, 2019; Hassan *et al.*, 2021); their states (active or relict) can be used in

30 Permafrost Zonation Index (PZI) models to predict the probability of permafrost occurrence where field observation data are scarce (Cao *et al.*, 2021; Boeckli *et al.*, 2012a). The large-scale distribution of active rock glaciers is influenced by the complex interaction of climatic and topographic factors (Schrott, 1996; Millar and Westfall, 2008; Pandey, 2019). Global climate change may affect the stability of rock glaciers and permafrost, thus impacting slope stability, runoff patterns and water quality, with possible consequences for periodic

35 landslides, debris flows, floods and other geological disasters (Barsch, 1996; Schoeneich *et al.*, 2015; Blöthe *et*

al., 2019; Hassan *et al.*, 2021). Exploring their spatial distribution and evolution is therefore significant for paleoclimatic modeling, disaster risk assessment and infrastructure maintenance (Arenson and Jakob, 2010; Colucci *et al.*, 2016; Selley *et al.*, 2018; Alcalá-Reygosa, 2019). Furthermore, the slow thawing process through heat diffusion with latent heat exchange at depth, combined with the cooling effect of the ventilated coarse

40   blocks at the surface of rock glaciers, make them a largely inert hydrological reserve in high mountain systems (Bolch and Marchenko, 2009; Berthling, 2011; Bonnaventure and Lamoureux, 2013; Millar and Westfall, 2013). The presence and abundance of rock glaciers can therefore affect the quantities and properties of runoff from high mountain watersheds over extended time periods (Jones *et al.*, 2019b).

      The Tibetan Plateau (TP) is among the key high-altitude areas of periglacial landform worldwide, and is a
45   region highly sensitive to climate change (Cui *et al.*, 2019; Yao *et al.*, 2019). Detailed rock glacier inventories have previously been constructed for the Gangdise Mountains (Zhang *et al.*, 2022), the Daxue Mountains (Ran and Liu, 2018), the Nyainqêntanglha Range (Reinosch *et al.*, 2021), and the Nepalese Himalaya (Jones *et al.*, 2018b). The Yarlung Zangbo River Basin (YZRB) is one of the regions with the highest concentrations of modern glaciers on the TP; it is experiencing rapid geomorphic evolution today (Ji *et al.*, 1999; Korup and
50   Montgomery, 2008; Yu *et al.*, 2011; Long *et al.*, 2022). Although Guo (2019) characterized the spatial distribution of rock glaciers in the YZRB using manual visual interpretation, there remains a lack of any systematic and detailed rock glacier inventory, and the regional occurrence characteristics and indicative environmental significance of these rock glaciers are still unclear. Even though ground-penetrating radar (GPR), seismic refraction tomography (SRT), electrical resistivity tomography (ERT) and other geophysical techniques
55   are widely used today and can provide new insights into understanding the ice volumes of rock glaciers and permafrost (Janke *et al.*, 2015; Emmert and Kneisel, 2017; Bolch *et al.*, 2019; Buckel *et al.*, 2021; Halla *et al.*, 2021; Mathys *et al.*, 2022), it remains difficult to apply such methods to large-scale field-based research on the TP. The distribution of permafrost and the hydrological contributions made by rock glaciers on the TP need more research.

60   To address this, our study aims to: (i) compile a more comprehensive and systematic inventory of rock glaciers in the GLKRJ; (ii) explore the regional occurrence characteristics and indicative environmental significance of these rock glaciers; (iii) assess the regional hydrological significance of rock glaciers and glaciers; and (iv) compare the distribution of the GLKRJ's rock glaciers to the regional permafrost maps.

2 Study area
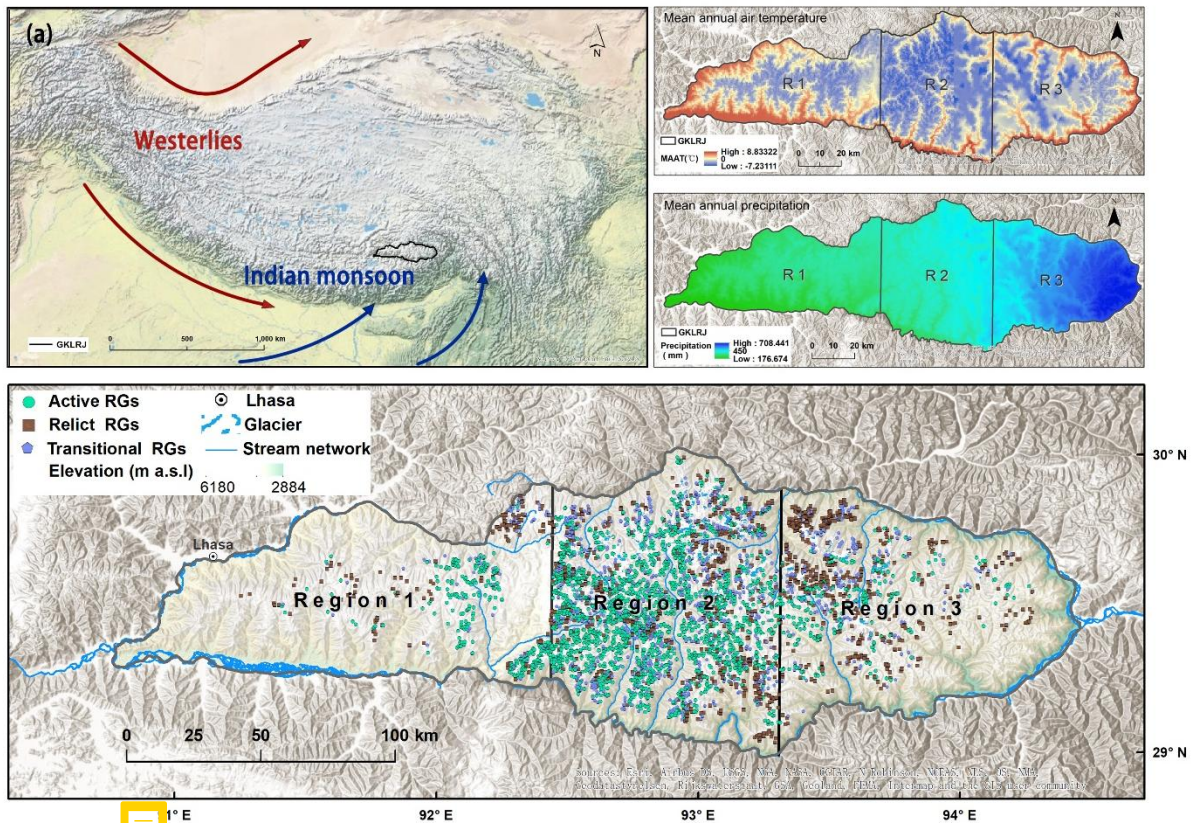
Figure 1: (a) The location of the GKLRJ on the TP; **(b)** The three sub-regions and the spatial distribution of streams. Rock glaciers are categorized as green (active rock glaciers), purple (transitional rock glaciers), brown (relict rock glaciers), and glaciers are shown in light blue and white; **(c)** Mean annual air temperature map for the GKLRJ (Du and Yi, 2019); **(d)** Mean annual precipitation map for the GKLRJ (Du and Yi, 2019). Maps were created using ArcGIS® software by Esri.

The GKLRJ region is located between 92.916°N – 93.276°N and 29.287°E – 29.438°E, on the southeastern TP, adjacent to the Himalayas to the south and the Nyainqêntanglha Range to the north (see Fig.1). It forms the eastern extension of the Gangdise Mountains as well as the watershed of the Yarlung Zangbo River and its tributary, the Niyang-Lhasa River, and belongs to the high mountain plateau-lake basin-wide valley area of the middle and upper reaches of the Yarlung Zangbo and Nujiang rivers (Xiang *et al.*, 2013). The region is also within the world's largest irrigated agricultural area and has a dense population (Yao *et al.*, 2022).

Tectonically, the GKLRJ is located in the eastern part of the Ladakh-Kailas-Xiachayu magmatic arc of the Gangdise-Himalayan collisional orogen; from the Late Paleozoic to the Mesozoic, it has experienced the same evolutionary tectonic processes as the Gangdise-Himalayan archipelagic arc-basin systems, *i.e.*, back-arc spreading, arc-arc collision and arc-continental collision (Pan *et al.*, 2013). The GKLRJ's main rock types include Late Cretaceous quartz monzonite, Eocene monzonite and Eocene biotite granite. It is located in the transition belt between the TP's semi-arid and humid regions (Zheng *et al.*, 2010), mainly dominated by the Indian Summer Monsoon (ISM). The middle and western parts of the GKLRJ belong to the TP's temperate, semi-arid zone, while the eastern part belongs to plateau's temperate humid region (Zheng *et al.*, 2010). The mean annual air temperature (MAAT) is -7.2 – 8.8ºC (Du and Yi, 2019), and the mean annual ground temperature (MAGT) is -3.2 – 4.5ºC (Ran *et al.*, 2020). The mean annual precipitation (MAP) is 177 – 708 mm, decreasing from east to west across the study area (Du and Yi, 2019) (see Table.1). Changes in the imbalance

between glaciers, permafrost, lakes and rivers in this region under the influence of climate change may lead to spatial and temporal changes in local ecosystems and changes in water resources in downstream areas (Yao *et al.*, 2022).

Table 1: MAAT (Du and Yi, 2019), MAGT (Ran *et al.*, 2020), MAP (Du and Yi, 2019), mean alitude(ASTER GDEM v3) and mean glacier ELA(Liu *et al.*, 2012)for the GKLRJ and its three sub-regions.

Region	MAAT (ºC)	MAGT (ºC)	MAP (mm)	Mean altitude (m asl)	Mean glacier ELA (m asl)
All	0.69	0.53	469	4,623	5,431
R1	1.78	1.65	385	4,589	5,484
R2	-0.63	-0.06	489	4,893	5,462
R3	0.91	0.01	534	4,398	5,292

MAGT: mean annual ground temperature
MAAT: mean annual air temperature
MAP: mean annual precipitation

We divided the GKLRJ into three sub-regions: R1(east); R2 (central); and R3(west). These divisions were geospatially based (see Fig.1b), where R1 and R2 are bounded by the eastern marginal rift valley of the Oiga Basin, and R2 and R3 are bounded by Niang River, a tributary of the Niyang River. Each sub-region displays unique characteristics in terms of its topography and climate (see Table 1). The whole of R1 is a semi-arid region, and the terrain is more complex here. The western side of R1 is composed of a deep alpine valley landscape formed by glacial-fluvial erosion cutting through the undulating terrain, while the eastern side is a basin formed by paleoglacial erosion and fluvial erosion cutting through less undulating mountainous hills with relatively gentle tops (Wu *et al.*, 2010). R2 is a semi-arid and semi-humid transition zone where the dividing line is located in its northeastern part; the mean altitude here is higher than in the other regions. The main peaks of glacier-carved mountains occur mostly above 5,500 m asl. R3 is located in a semi-humid zone where precipitation is more abundant and the terrain is on average ~500 m lower than that of R2.

3 Material and methods

3.1 Rock glacier inventory, classification and database

We used high-resolution ©Google Earth Pro remote sensing images from March 2004 to August 2020 to manually and visually interpret and compile a rock glaciers inventory for the GKLRJ (Selley *et al.*, 2018; Magori *et al.,* 2020; Hassan *et al.,* 2021). The inventorying strategy follows the RGI_PCv2.0 (RGIK, 2022b). According to the technical definition of rock glaciers, we conducted the detection of rock glacier landforms in the study area and confirmed the relevant landforms (system/unit). For areas with missing clear imagery and those covered by snow, we simultaneously used the ©Map World for comparison and verification, ensuring that all outline segments can be labeled with certainty. Each cataloged rock glacier system/unit was assigned a primary ID and delineated according to the extended standards, with the outline encompassing the entire rock glacier up to the rooting zone, including its external parts such as the front and lateral margins (RGIK, 2022b). We followed as closely as possible the specific rules for delineating the upper boundaries of the rock glacier and provided information on their upslope connection type in the attribute table (RGIK, 2022a, 2022b). Due to the limited availability of accurate field observations and related data on rock glacier dynamics, their activity states were determined solely based on geomorphological criteria (RGIK, 2022a). The activity type of each rock glacier was recorded in the attribute table.
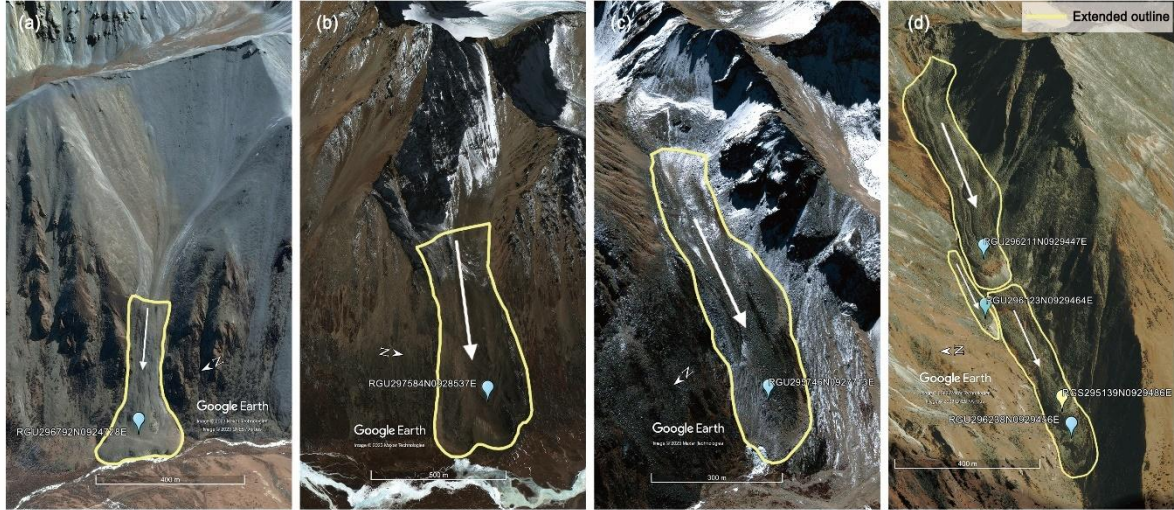
Figure 2: Example images of different upslope boundary types of rock glaciers in the GKLRJ. (a) a deris-mantled slope-connected rock glacier; (b) a talus-connected rock glacier; (c) a glacier forefield-connected rock glacier; (d) a rock glacier system. Images from ©Google Earth.

3.2 Estimating hydrological stores

To calculate more accurately the water content (water volume equivalent, WVEQ [km^3]) of the perennially frozen rock glaciers (including active and transitional rock glaciers) and of surface ice in glaciers in the GKLRJ (Jones *et al.*, 2018b), we chose two different methods derived from Brenning *et al.* (2005a) and Cicoira *et al.* (2021).

The method for calculating the subsurface ice volumes of rock glaciers permafrost provided by Brenning *et al.* (2005a) requires multiplying the mean thickness, surface area and ice content of each rock glacier as in Eq. (1), then converting them to the WVEQ by assuming an ice density conversion factor of 0.9 g cm^{-3} ($\equiv$ 900 kg m^{-3}) (Paterson, 1994; Jones *et al.*, 2018b), thus:

$$V_{RG} = \text{Area} * \text{Mean thickness} * \text{Ice Content} \tag{1}$$

Based on field data from Brenning *et al.* (2005a) and a rule-of-thumb given by Barsch (1977c) for the Swiss Alps, the rock glacier thickness was modeled empirically as Eq. (2), thus:

$$\text{Mean thickness [m]} = 50 * (\text{Area [km}^2])^{0.2} \tag{2}$$

The method provided by Cicoira *et al.* (2021), based on the analysis of a dataset of 28 rock glaciers from the Alps (23) and the Andes (5), estimated rock glacier thickness using a perfectly plastic model arrived at by solving Eq. (4) for *H*, assuming a yield stress of τ = 92 kPa (taking the mean driving stress from the dataset as a given), thus:

$$H = \frac{\tau}{\rho \, g \, sin\alpha} \pm 3.4m \tag{3}$$

where τ is the sheer stress (τ= 92 kPa), *g* is the gravitational acceleration, *H* is the thickness of the moving rock glacier, α is the angle of the surface slope and ρ is the density of the creeping material, which is given by the contribution of volumetric debris w_d and ice content w_i and the relative densities (ρ_i = 910 kg m^{-3} and ρ_d = 2700 km m^{-3}), thus:

$$\rho = \rho_d \, w_d + \rho_i \, w_i \tag{4}$$

The ice content in rock glacier permafrost is spatially variable. We therefore used global estimates of ice content within rock glacier to further calculate their lower (40%), mean (50%) and upper (60%) ice volumes

(Hausmann *et al.*, 2012; Krainer and Ribis, 2012; Rangecroft *et al.*, 2015; Jones *et al.*, 2018b; Wagner *et al.*, 2021). In this study, the results of the calculations that used a 50% ice content were used for subsequent comparisons with the surface ice in glaciers.

The ice volume of glacier was calculated using Eq. (5), thus:

$$V = A * H \ , \tag{5}$$

where *V* represents ice volume, *A* is the glacier surface area derived from the second Chinese glacier inventory (version 1.0) (2006-2011) (Liu *et al.*, 2012), and *H* is the ice thickness calculated using GlabTop2 in Python 3.10 (Linsbauer *et al.*, 2009). We assumed a 100% ice content by volume and applied the above ice density conversion factor to calculate the water equivalent volume of the surface ice in glaciers.

To mitigate the additional impact caused by the uneven spatial distribution of glaciers and rock glaciers in the GKLRJ, we calculated a ratio of rock glaciers (including active and transitional rock glaciers)' to glaciers' water volume equivalence (WVEQ) by using the weighted average method that employs the following equation:

$$\text{WVEQ ratio}_{\text{Rg: Glacier}} = \frac{\text{WVEQ R1}_{\text{Rg}} \times \frac{\text{R1}_{\text{Rg}}}{\text{All}_{\text{Rg}}} + \text{WVEQ R2}_{\text{Rg}} \times \frac{\text{R2}_{\text{Rg}}}{\text{All}_{\text{Rg}}} + \text{WVEQ R3}_{\text{Rg}} \times \frac{\text{R3}_{\text{Rg}}}{\text{All}_{\text{Rg}}}}{\text{WVEQ R1}_{\text{Glacier}} \times \frac{\text{R1}_{\text{Glacier}}}{\text{All}_{\text{Glacier}}} + \text{WVEQ R2}_{\text{Glacier}} \times \frac{\text{R2}_{\text{Glacier}}}{\text{All}_{\text{Glacier}}} + \text{WVEQ R3}_{\text{Glacier}} \times \frac{\text{R3}_{\text{Glacier}}}{\text{All}_{\text{Glacier}}}} \tag{6}$$

where WVEQ ratio$_{\text{Rg: Glacier}}$ is the ratio of rock glaciers' to glaciers' WEVQ; WVEQ Rn$_{\text{Rg}}$ (n = 1, 2, 3) are the WVEQ values for rock glaciers in R1, R2 and R3, respectively; Rn$_{\text{Rg}}$ (n = 1, 2, 3) are the numbers of rock glaciers in R1, R2 and R3, respectively; All$_{\text{Rg}}$ is the number of rock glaciers in the whole GKLRJ; WVEQ Rn$_{\text{Glacier}}$ (n = 1, 2, 3) are the WVEQ values for glaciers in R1, R2 and R3, respectively; Rn$_{\text{Glacier}}$ (n = 1, 2, 3) are the number of glaciers in R1, R2 and R3, respectively; and All$_{\text{Glacier}}$ is the number of glaciers in the whole GKLRJ.

4 Results

4.1 Rock glacier inventory analysis
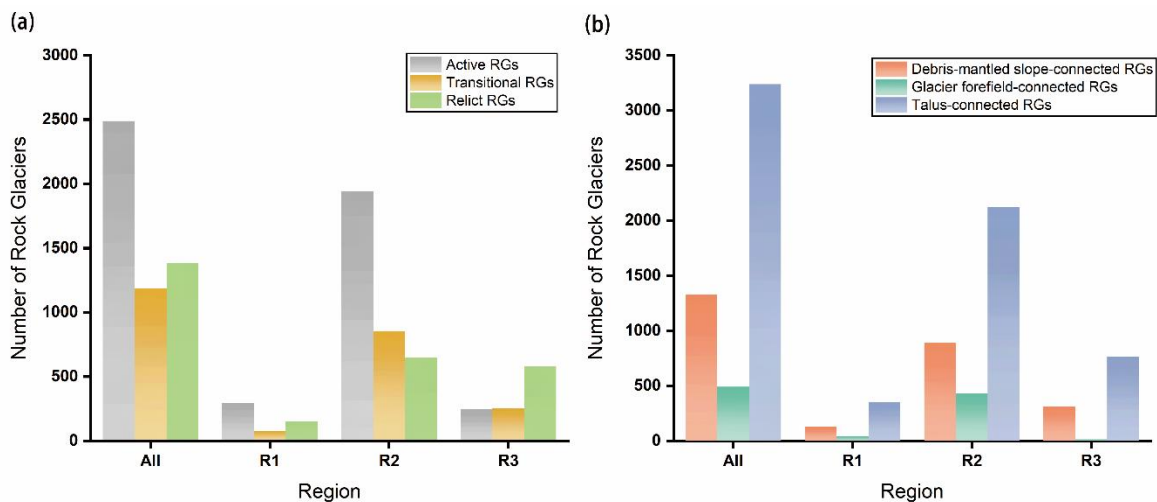
Figure 3: The number of rock glaciers categorized by different types of activity and upper slope connection in the entire GKRLJ and its sub-regions.

We identified a total of 5,057 rock glaciers in the GKLRJ, including 2,484 active rock glaciers (49.1%), 1,189 transitional rock glaciers (23.5%), 1,384 relict rock glaciers (27.3%). Active rock glaciers are predominant in the whole GKLRJ, with the exception of R3 where a higher proportion of relict rock glaciers can be found

(Fig. 3a). Among the total rock glaciers observed, ~64% of them (n = 3,239) were classified as talus-connected, ~26% (n = 1,327) as debris-mantled slope-connected, and ~10% (n = 491) as glacier forefield-connected, this order of proportions is consistent across three subregions. On the whole, rock glaciers are unevenly distributed in R1, R2 and R3, with nearly 70% of rock glaciers (n = 3,447) distributed in R2 (see Table 4).
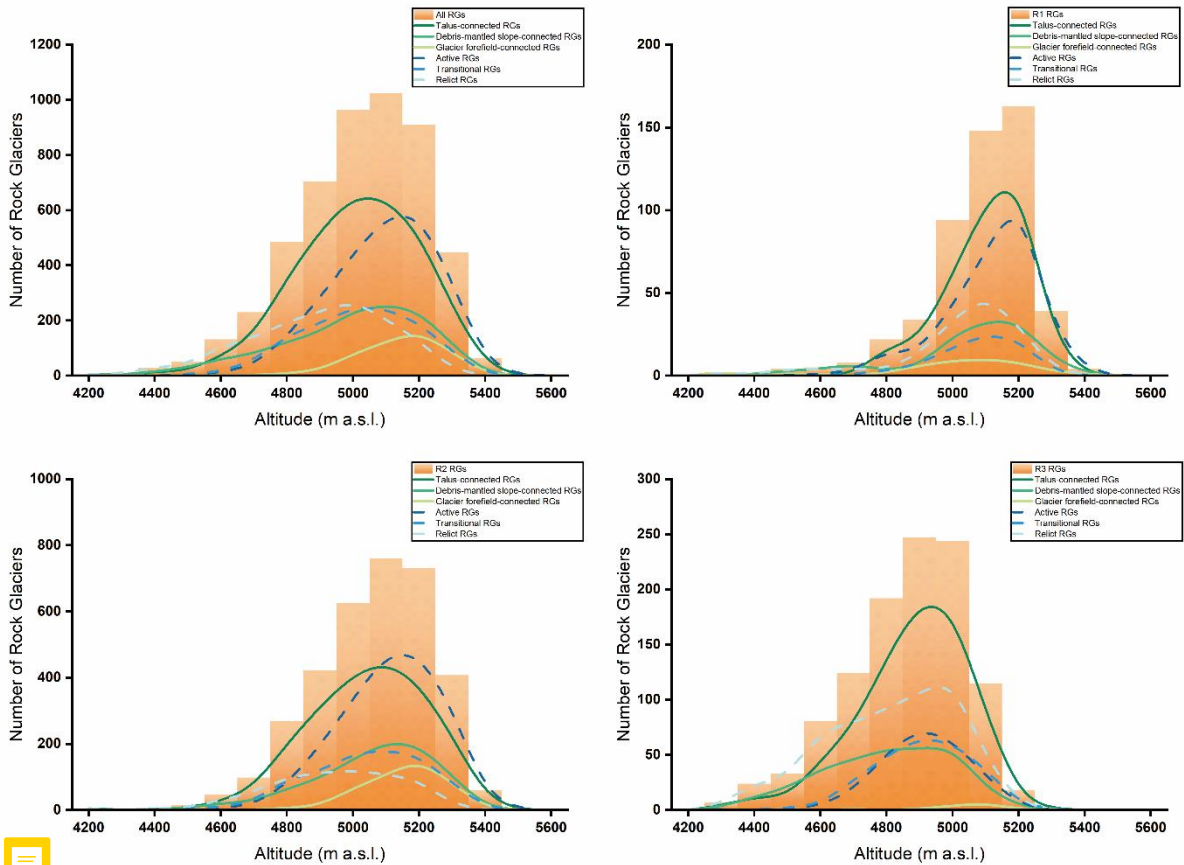
Figure 4: The mean occurrence altitude of rock glaciers categorized by different activity and upper slope connection types in (a)the whole GKLRJ and (b)R1, (c)R2 and (d)R3.

~90% of the rock glaciers are located between 4,800 and 5,400 m asl, with a mean altitude of ~5,070 m asl. Active rock glaciers are statistically distributed at higher altitudes than transitional and relict rock glaciers (ANOVA: F-value = 544.749, df within groups = 2, between groups = 5,054, p ⩽ 0.001) , at ~76 m and ~195 m higher. The mean alititude of rock glaciers varies significantly depending on the type of spatial connection to the upper slope (ANOVA: F-value = 102.9, df within groups = 2, between groups = 5,054, p ⩽ 0.001). Compared to talus-connected (~5,063 m asl) and debris-mantled slope-connected rock glaciers (~5,044 m asl), glacier forefield-connected rock glaciers (~5,185 m asl) are more commonly found at higher elevations. The mean altitude of rock glaciers in R1 (~5,132 m asl) is higher than for those in R2 (~5,112 m asl) and R3 (~4,909 m asl) by ~20 m and ~223 m, respectively (see Table 4). The lower altitudinal limit of rock glaciers declines as longitude increases eastward (see Fig. 5).
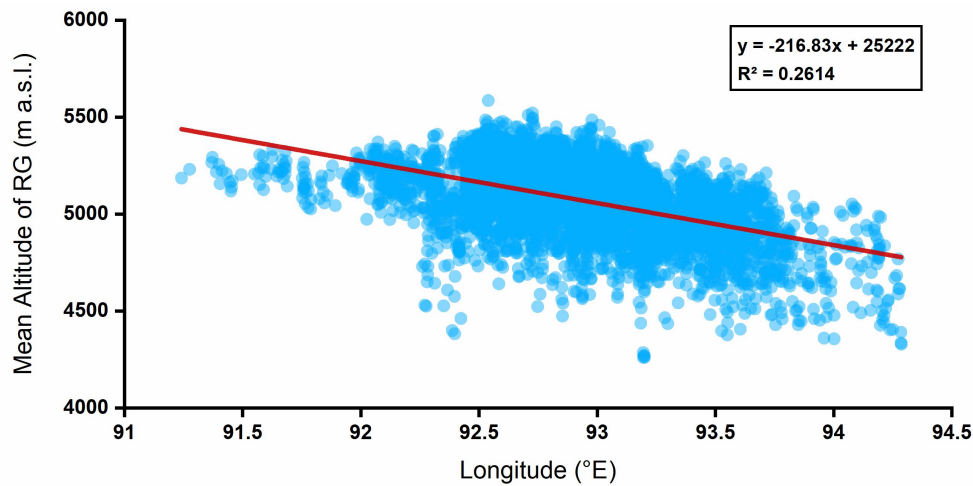
Figure 5: Scatterplots and fitted curves of the mean altitudinal distribution of rock glaciers versus longitude.

In the GKLRJ, rock glaciers cover an area of 404.69 km^2, with the mean area of each rock glacier being 0.08 km^2, the mena area of three different activity types of rock glaciers remains consistent with this value, but there are notable variations in the mean area of rock glaciers depending on their specific type of upper slope connection (ANOVA: F-value = 89.814, df within groups = 2, between groups = 5,054, $p \leqslant 0.001$). Glacier forefield-connected rock glaciers (0.12 km^2) generally have a larger mean area than the talus-connected ones (0.08 km^2) and the debris-mantled slope-connected ones (0.06 km^2). The mean area of most types of rock glacier is the biggest in R2 and smallest in R1 (Table.4). Furthermore, the mean slope range of rock glaciers in R3 is significantly steeper compared to that in R1 and R2 (ANOVA: F-value = 81.175, df within groups = 2, between groups = 4,680, $p \leqslant 0.001$).

Table 4: Mean characteristics for rock glaciers.

Type	R1	R2	R3
Number	524	3,447	1,086
Mean altitude (m asl)	5,132	5,117	4,909
Mean MEF (m asl)	5,083	5,051	4,845
Mean area (km^3)	0.06	0.08	0.07
Mean slope range (°)	19.85	19.23	21.43
Mean MAGT (ºC)	-0.02	-0.6	-0.9
Mean MAAT (ºC)	-1.68	-1.94	-1.54
Mean MAP (mm)	343	392	495

MEF: minimum altitude at the rock glacier front
MAGT: mean annual ground temperature
MAAT: mean annual air temperature
MAP: mean annual precipitation
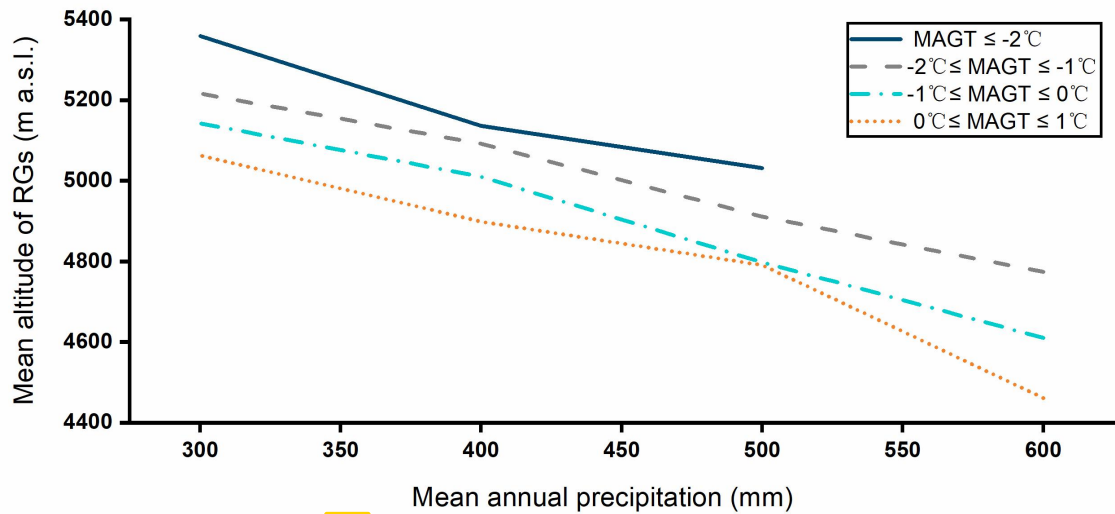
Figure 6: The variation in rock glacier distribution altitude with changes in precipitation for different MAGT states.

Around 90% of the rock glaciers in GKLRJ are found in the region where the MAGT ranges from -2°C to 0°C. Additionally, the MAGT, MAAT and MAP of the rock glaciers vary among the three sub-regions (Table.4). Specifically, the mean MAGT decreases gradually from R1 to R3, while the mean MAP increases gradually. The mean MAAT follows the same order as the regional mean MAAT values listed in Table 1. With the same MAGT, the mean altitude of rock glacier distribution decreases with increasing MAP. Moreover, with the same MAP, the altitude of rock glacier distribution increases with decreasing MAGT (Fig.6).
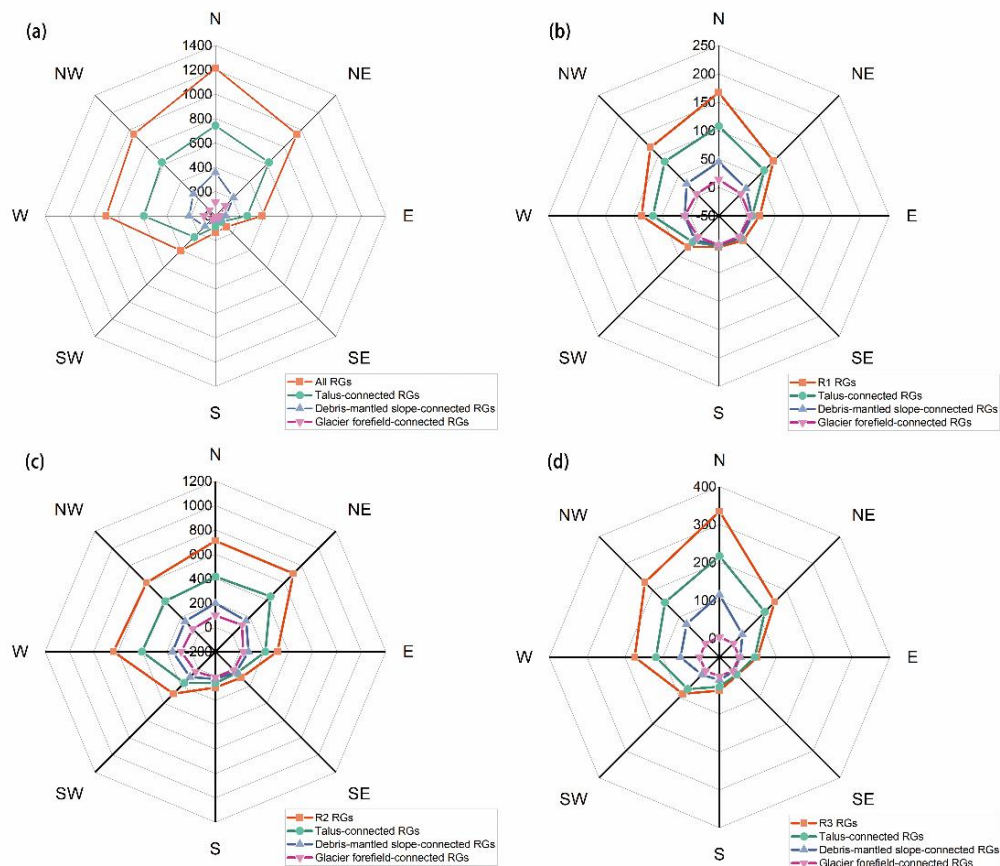
Figure 7:   Analysis of abundances for different rock glacier activity states. The numbers of rock glaciers for each aspect on the four radar plots are shown as percentages (%).

Rock glaciers predominantly occur on north-facing slopes (N, 23.9%; NW, 18.7%; NE, 18.7%), with some

distributed on the west-facing aspects (W, 17.7%), and fewest on south-facing aspects (S, 2.7%; SE, 2.5%, SW, 7.9%) (see Fig. 5). Compared with the obvious characteristics of the concentrated distribution of rock glaciers in R1 and R3 on the N aspect, rock glaciers in R2 are more evenly distributed on the N, NE, W and NW aspects.

4.2 Water equivalent volumes

Based on the second Chinese glacier inventory (Liu *et al.*, 2012), glaciers in the GKLRJ cover an area of ~372.32 km^2. GlabTop2 provided estimated clean ice glacier thicknesses ranging between ~1 and ~263 m (mean = ~18 m). We estimated the total WVEQ of the region's glaciers to be ~9.29 km^3.

Table 5: Ice volumes (km^3) and corresponding WVEQs (km^3) calculated using the empirical area-thickness formula (Brenning, 2005a) for sub-regions and GKLRJ-wide (All).

Brenning, 2005a					
Region	Glacier - WVEQ (km^3)	RG - WVEQ (km^3)			RG: Glacier WVEQ ratio
		40%	50%	60%	
All	9.29	3.45	4.32	5.18	1:2.28
1	0.19	0.30	0.38	0.45	2:1
2	6.60	2.78	3.47	4.17	1:1.9
3	2.51	0.36	0.46	0.55	1:5.5

WVEQ = water volume equivalent

The mean thickness of rock glaciers in the GKLRJ estimated using the empirical area-thickness formula (Brenning, 2005a) is ~28.35 m. The WVEQ storage lies between 3.45 and 5.18 km^3, of which R2 stores ~80% of the water in the GKLRJ (*i.e.*, 2.78 – 4.17 km^3). R1 stores 0.30 – 0.45 km^3 of water (9% of the whole GKLRJ reserve). R3 stores ~11% of the water, or 0.36 – 0.55 km^3(see Table 5). Compared to the WVEQ of glaciers, the result calculated using the weighted method showed that the ratio was 1:2.28, indicating that glaciers stored ~ 2.28 times more water than rock glaciers.

Table 6: Ice volumes (km^3) and corresponding WVEQs (km^3) calculated using the perfectly plastic model (Cicoira *et al.*, 2021) for sub-regions and GKLRJ-wide (All).

Cicoira *et al.*, 2021					
Region	Glacier - WVEQ (km^3)	RG - WVEQ (km^3)			RG: Glacier WVEQ ratio
		40%	50%	60%	
All	9.29	1.31 – 2.02	1.64 – 2.53	1.97 – 3.04	1:4.66
1	0.19	0.11 – 0.17	0.14 – 0.22	0.17 – 0.26	1:1.06
2	6.60	1.08 – 1.65	1.35 – 2.06	1.62 – 2.48	1:3.86
3	2.51	0.11 – 0.19	0.14 – 0.24	0.17 – 0.29	1:13.21

WVEQ = water volume equivalent
The range of results in RG - WVEQ (km^3) (Cicoira *et al.*, 2021) corresponds to $H\pm3.4$ m.

The mean thickness of rock glaciers calculated using a perfectly plastic model (Cicoira *et al.*, 2021) is 16.39±3.4 m, 11.96 m thinner than that estimated using the empirical area-thickness formula. The mean value of the WVEQ estimated using this method is 41 – 49% of the mean value obtained using the 'Brenning' method. As the estimated WVEQ of rock glaciers decreases, the ratio of rock glaciers' to glaciers' WVEQ is also lower than that obtained using the 'Brenning' method (Brenning, 2005a), indicating that the WVEQ of glaciers is ~4.66 times that of rock glaciers (see Table 6).

5 Discussion

5.1 Factors controlling rock glaciers

Rock glaciers are distributed heterogeneously throughout the GKRLJ, with most concentrated within R2. The GKLRJ spans a large area from east to west, with variations in topography and climatic conditions between the three sub-regions, thereby providing the basis for a spatially differentiated distribution of rock glaciers. The development of rock glaciers is a complex function of responses to air temperature, insolation, wind and seasonal precipitation over a considerable time period (Humlum, 1998), with the MAAT = -2°C isotherm and the equilibrium line altitude (ELA) for local glaciers forming the lower and upper boundaries of the cryogenic belt where they have developed, respectively (Humlum, 1988; Brenning, 2005a; Rangecroft *et al.*, 2015, 2016; Jones, 2018b). Topographically, the higher terrain in R2 has accommodated the development of more rock glaciers in the area above 4,500 m asl. R2 is located in the transition zone between the TP's semi-arid and sub-humid regions, with a mean ELA of ~5,462 m asl. Compared with R3, which has a lower ELA (mean ELA = 5,292 m asl), and R1, which has a higher MAAT, R2 exhibits a broader range of the cryogenic belt to meet the development and distribution of more rock glaciers. Additionally, the widespread glacial remains in R2 and the predominance of more easily weathered granite as bedrock in this area could also provide a richer source of material for rock glacier development (Wahrhaftig and Cox, 1959; Haeberli *et al.*, 2006).

The mean and lower altitudinal limits of the rock glacier distribution in the GKLRJ decrease from west to east, from ~5,200 m asl to ~4,900 m asl. In the Gangdise Mountains, located in the same latitudinal range on the western side of the study area, rock glaciers show a similar trend of gradually decreasing altitude in line with increased moisture; indeed, the characteristics of the changes in the two regions show an overall continuity (Zhang *et al.*, 2022). Limited by the range of the ISM, MAP gradually decreases from west to east from the Gangdise Mountains to the GKLRJ. In the alpine tundra of this region, annual precipitation is dominated by snowfall in summer and autumn. Increases in snowfall in summer and autumn could help to preserve permafrost, allowing permafrost to develop at lower altitudes under similar climatic conditions (Zhou *et al.,* 2000). Additionally, annual regional precipitation values may reflect reductions in short-wave insolation arising from cloud cover, at least to some extent (Boeckli *et al.*, 2012a). Relatively favorable hydrological conditions will be more conducive to freeze-thaw weathering, thereby increasing the generation rate of rock debris, which in turn is conducive to the development of rock glaciers (Hallet *et al.*, 1991; Haeberli *et al.*, 2006; Zhang *et al.*, 2022). Increases in MAP are therefore likely to be conducive to the expansion of the range in the distribution of rock glaciers in semi-arid to sub-humid areas, meaning that the lower altitudinal limit of rock glacier distribution decreases with increases in annual precipitation.

Glacier forefield-connected rock glaciers may have a more abundant source of materials comparing to other types of rock glaciers. They distributed in regions where glaciers have previously existed, and both glacial moraines and surrounding rock walls can provide debris as their materials. Therefore, they have a more diverse range of material sources, which may contribute to the development of larger-scale rock glaciers. However, debris-mantled slope-connected rock glaciers lack significant headwall, and their debris is primarily produced by in-situ bedrock weathering (RGIK, 2022a). This results in their relatively limited and homogeneous material sources, leading to slower development and smaller scale compared to other types of rock glaciers.

Rock glaciers in GKLRJ are primarily distributed on north-facing and west-facing aspects, which is

remarkably similar to the distribution pattern of rock glaciers in the Himalayas (Jones *et al.*, 2018b), Gangdise Mountains (Zhang *et al.*, 2022), Tianshan Mountains (Liu *et al.*, 1995; Bolch and Marchenko, 2009) and the European Alps (Scotti *et al.*, 2013). This is mainly due to the fact that north-facing slopes receive less solar radiation as they are shaded, providing favorable conditions for the development and preservation of rock glaciers (Barsch, 1996). Additionally, the ample space and lower potential incoming solar radiation (PISR) on west-facing slopes, influenced by regional topographic conditions, also contribute to the development of rock glaciers here. This is evident in R2 where rock glaciers are more evenly distributed in the W, NW, N, and NE aspects compared to the distinct concentration of rock glaciers on the N aspect in R1 and R3.

5.2 Hydrological significance of rock glaciers

In comparison, we found that the thicknesses of rock glaciers calculated using the flow plasticity model (Cicoira *et al.*, 2021) are significantly lower than the corresponding results calculated using the empirical area-thickness formula (Brenning, 2005a). By comparing the thickness of the rock glaciers calculated by both methods with the height of the rock glacier front measured in© Google Earth, the thickness of the rock glaciers calculated by the 'Cicoira' method (Cicoira *et al.*, 2021) seems to be closer to the real value. Therefore, we speculate that the thickness calculated based on the 'Brenning' method (Brenning, 2005a) may be overestimated to a certain extent   due to the following reason. The applicability of different estimation methods may be different across the study area. The mean thickness of the sample rock glaciers in the study of Brenning (2005a) about 30-50 m, which are higher than the sample of rock glaciers selected in the study of Cicoira *et al.* (2021) (15-30 m). We selected two rock glacier samples from Cicoira *et al.*'s (2021) research and used the 'Brenning' method (Brenning, 2005a) to calculate their thickness (Müller *et al.*, 2016). We observed that the calculated thickness (H=27 m) closely matched the actual thickness for the rock glacier with an area of 45,931 m^2 and a real thickness of 30 m. However, there was a significant discrepancy with the other rock glacier sample (H=25 m), which had an area of 32,356 m^2 and an actual thickness of 12 m. Therefore, the applicability of empirical formulaes based on various samples may vary for estimating the thickness of rock glaciers in different areas. As the thickness of rock glaciers in GKLRJ is relatively close to the sample selected by Cicoira *et al.* (2021), the application of the Brenning' method (Brenning, 2005a) may lead to an overestimation of rock glacier thickness in GKLRJ.

Based on the above discussion, we choose to use the results calculated based on the Cicoira' method (Cicoira *et al.*, 2021), which may be closer to the actual water reserves in GKLRJ for further comparison and discussion. These estimates indicate that the amount of water stored in rock glaciers in the GKLRJ is ~3.5% of the total previously-identified rock glacier water reserves globally (94.66 Gt), and ~2.2% of the existing water reserves in rock glaciers on the TP (58.05 Gt) (Jones *et al.*, 2018a; Jones *et al.*, 2018b; Jones *et al.*, 2021). The rock glacier to glacier storage ratio in the GKJRJ of 1:4.66 is ~133 times bigger than the global ratio (1:618, excluding the Antarctic and Subantarctic and Greenland Periphery Randolph Glacier Inventory) (Randolf Glacier Inventory (RGI); Pfeffer *et al.*, 2014; Jones *et al.*, 2018a), ~5.4 times bigger than that of the Himalayas to its south (1:25) (Jones *et al.*, 2021), and much closer to that of the Andes in South America (1:3) (Azócar and Brenning, 2010), where glacier presence is also limited/absent (Brenning, 2005b; Azócar and Brenning, 2010; Jones *et al.*, 2019b; Schaffer *et al.*, 2019). In the GKLRJ, regional differences in the hydrological significance of rock glaciers under different climatic conditions also exist (ANOVA: *F*-value =27.930, df within groups = 2,

between groups = 3,671, $p \leqslant 0.001$). In R2, which is located in the transition zone between the semi-arid and semi-humid zones, the higher topography and suitable hydrothermal conditions lead to the highest concentration of glaciers and rock glaciers in this area, with rock glaciers accounting for 82% of the rock glacier water storage in the entire study area, and glaciers accounting for ~71% of the study area's glacial water storage, with a ratio of ~1:3.86 between them. However, in terms of the ratio of rock glaciers to glacial water storage alone, rock glaciers are of greater hydrological significance in the warmer and drier R1, despite it storing only 8.7% of the total water volume of all rock glaciers. In the context of drought and climate warming, rock glaciers store more than twice the water of the glaciers in R1. This partly explains why rock glaciers have a greater hydrological significance and refuge potential as long-term reservoirs in arid regions with small and rapidly vanishing glaciers. Furthermore, the relationship between the proportion of the water cycle occupied by rock glaciers and the water requirements of regional populations should be considered in more detail. More research is needed into the hydrochemical composition of the stored water in rock glaciers and whether it can be used for irrigation and drinking.

5.3 Rock glaciers and permafrost presence
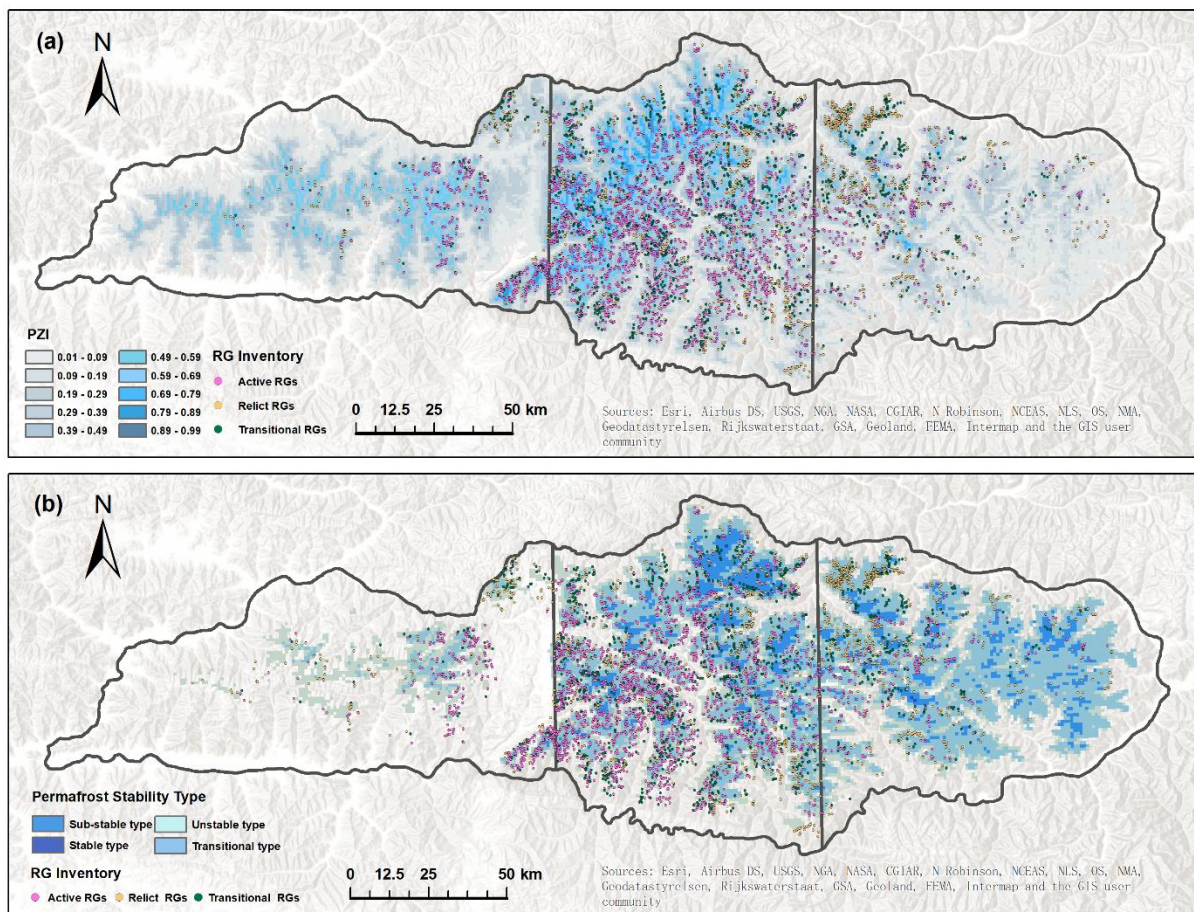
Figure 8: Spatial distribution of rock glaciers vs. (a) Gruber's (2012) Permafrost Zonation Index (PZI) in GKLRJ and (b) Map of the thermal stability of permafrost in GKLRJ (Ran _et al._, 2020).

The MAGT in GKLRJ is relatively high (Ran _et al._, 2020; Ni _et al._, 2020). Approximately 90% of the rock glaciers are distributed within the MAGT range of -2°C to 0°C, which belong to the regions of sub-stable type ($-3°C < MAGT < -1.5°C$), transitional type ($-1.5°C < MAGT < -0.5°C$), and unstable type permafrost ($-0.5°C$

< MAGT < 0.5°C) (Cheng *et al.*, 2019). And about 7% of the rock glaciers occur in the seasonal frozen ground area with MAGT > 0°C. Overall, the distribution of rock glaciers in GKLRJ aligns well with the regions of Permafrost Zonation Index (PZI)≥0.49 in map provided by Gruber (2012) and the map of the thermal stability of permafrost provided by Ran *et al.* (2020), especially in R2 and the western part of R3. In R1, the range of permafrost distribution provided by Ran *et al.* (2020) is significantly smaller than the region with PZI ≥ 0.49 in Gruber (2012), while in the eastern part of R3 is larger. We speculate that these differences may be attributed to variations in the data period used in these studies. When making detailed comparisons between the mean MAAT data from 1961 to 1990 used in the study of Gruber (2012) and MAAT data for the TP in 2015 provided by Du and Yi (2019), we found that, except for a few areas in the eastern part of R3, the mean MAATs of R1 and R2 increased by ~2°C. Although there may have been some errors in the data, the effect of temperature on the predicted permafrost distribution for the model based on the relationship between air temperature and the occurrence of permafrost may nonetheless be somewhat magnified.

With future climate warming, the permafrost located in the eastern part of the Tibetan Plateau with lower ground temperatures may experience a faster warming rate (Cheng *et al.*, 2019). This could result in rapid changes in the movement speed and surface morphology of rock glaciers in GKLRJ over a short period of time (Krainer and Mostler, 2006; Ikeda *et al.*, 2008; Janke and Bolch, 2021). However, research has shown that despite the relatively rapid increase in ground temperatures in the deep layers of permafrost, the thawing of permafrost on the Tibetan Plateau occurs at a slow pace with full consideration of deep ground temperatures, subterranean ice and geothermal gradients in permafrost (Cheng *et al.*, 2019). It may take centuries, if not millennia, for the frozen material and corresponding subsurface ice in rock glaciers and permafrost to completely thaw and melt (Krainer *et al.*, 2015).

6 Conclusions

We constructed an inventory of rock glaciers in the GKLRJ and illustrated their regional distribution characteristics and environmental indications. We employed two methods to estimate and compare the water storage capacity of the region's rock glaciers and map the GKLRJ's permafrost probability distribution using the logistic regression model. The results show that there are 5,057 rock glaciers in the GKLRJ, covering an area of 404.69 km^2. Over 80% of these rock glaciers are located within R2. The high altitude (~4,900 m asl), low temperatures (MAAT ≤ -2°C) and suitable precipitation (MAP ~400 mm) in the semi-arid and semi-humid transition zone provide the widest cryogenic belt range for rock glacier distribution in the region. The lower altitudinal limit of the distribution of rock glaciers decreases gradually with increasing longitude from the western side of the study area, from the Gangdise Mountains to the interior of the GKLRJ, indicating the positive effect of increased precipitation on the preservation of permafrost. We used two methods to estimate the thickness of rock glaciers and found that the results calculated based on the perfect plasticity model were more consistent with the actual situation in GKLRJ. Based on the result, we calculated that 1.31 – 3.04 km^3 of water is stored in the rock glaciers, or ~33% of the water presently stored in surface ice of glaciers. Despite these differences, both of these results reveal the previously neglected and important hydrological value of rock glaciers in the GKLRJ, particularly in R1, which is the drier sub-region. The WVEQ in rock glaciers and the ratio of subsurface ice in rock glacier permafrost to surface ice in glaciers may continue to increase with global

warming and as glaciers retreat in the future. And the stability of permafrost in the area of rock glacier distribution is likely to further decline.

Data availability. The data associated with this article can be found in the Supplementary Materials. These data include the Google maps of the most important areas described in this article, as well as a tabulation of the parameters of the rock glaciers found in the GKLRJ.

Author contributions. ML and GL designed the research. ML performed the analysis and wrote the paper. YY and ZP provided overall supervision and contributed to the writing.

Competing interests. The authors declare that they have no conflict of interest.

Acknowledgments. This work was supported by the Second Tibetan Plateau Scientific Expedition and Research (STEP; Grant 299 no. 2019QZKK0205).

References

Alcalá-Reygosa, J.: Rock glaciers of the mountains of Mexico; a review of current knowledge and paleoclimatic implications, Journal of South American Earth Sciences, 96, 10.1016/j.jsames.2019.102321, 2019.

Arenson, L. U. and Jakob, M.: The Significance of Rock Glaciers in the Dry Andes - A Discussion of Azocar and Brenning (2010) and Brenning and Azocar (2010), Permafrost and Periglacial Processes, 21, 282-285, 10.1002/ppp.693, 2010.

Azocar, G. F. and Brenning, A.: Hydrological and Geomorphological Significance of Rock Glaciers in the Dry Andes, Chile (27 degrees-33 degrees S), Permafrost and Periglacial Processes, 21, 42-53, 10.1002/ppp.669, 2010.

Baral, P., Haq, M. A., and Yaragal, S.: Assessment of rock glaciers and permafrost distribution in Uttarakhand, India, Permafrost and Periglacial Processes, 31, 31-56, 10.1002/ppp.2008, 2019.

Baroni, C., Carton, A., and Seppi, R.: Distribution and behaviour of rock glaciers in the Adamello–Presanella Massif (Italian Alps), Permafrost and Periglacial Processes, 15, 243–259, https://doi.org/10.1002/ppp.497, 2004.

Barsch, D.: Eine A Eine Abschätzung von Schuttproduktion und Schutttransport im Bereich aktiver Blockgletscher der Schweizer Alpen. GéoProdig, portail d'information géographique, 28:148–160, 1977c.

Barsch, D.: Permafrost creep and rock glaciers, Permafrost and Periglacial Processes, 3, 175-188, https://doi.org/10.1002/ppp.3430030303, 1992.

Barsch, D.: Rockglaciers: Indicators for the Present and Former Geoecology in High Mountain Environments, Springer-Verlag, Berlin, pp. 331, 10.2307/3060377, 1996.

Berthling, I.: Beyond confusion: Rock glaciers as cryo-conditioned landforms, Geomorphology, 131, 98-106, 10.1016/j.geomorph.2011.05.002, 2011.

Blöthe, J. H., Rosenwinkel, S., Höser, T., and Korup, O.: Rock-glacier dams in High Asia, Earth Surface Processes and Landforms, 44, 808-824, 10.1002/esp.4532, 2019.

Boeckli, L., Brenning, A., Gruber, S., and Noetzli, J.: A statistical approach to modelling permafrost distribution in the European Alps or similar mountain ranges, The Cryosphere, 6, 125-140, 10.5194/tc-6-125-2012, 2012a.

425   Bolch, T. and Marchenko, S.: Significance of glaciers, rockglaciers and ice-rich permafrost in the Northern Tien Shan as water towers under climate change conditions, Selected Papers from the Workshop in Almaty, Kazakhstan, 2006, 8, 132–144, 2009.

Bolch, T., Rohrbach, N., Kutuzov, S., Robson, B. A., and Osmonov, A.: Occurrence, evolution and ice content of ice-debris complexes in the Ak-Shiirak, Central Tien Shan revealed by geophysical and remotely-sensed

430   investigations, Earth Surface Processes and Landforms, 44, 129–143, https://doi.org/10.1002/esp.4487, 2019.

Bonnaventure, P. P. and Lamoureux, S. F.: The active layer: A conceptual review of monitoring, modelling techniques and changes in a warming climate, Progress in Physical Geography-Earth and Environment, 37, 352-376, 10.1177/0309133313478314, 2013.

Brardinoni, F., Scotti, R., Sailer, R., and Mair, V.: Evaluating sources of uncertainty and variability in rock

435   glacier inventories, Earth Surface Processes and Landforms, 44, 2450-2466, 10.1002/esp.4674, 2019.

Brenning, A.: Climatic and geomorphological controls of rock glaciers in the Andes of Central Chile: Combining Statistical Modelling and Field Mapping. Humboldt-Universität zu Berlin, Berlin, Germany, 2005a.

Brenning, A.: Geomorphological, hydrological and climatic significance of rock glaciers in the Andes of Central Chile (33-35 degrees S), Permafrost and Periglacial Processes, 16, 231-240, 10.1002/ppp.528, 2005b.

440   Buckel, J., Reinosch, E., Hördt, A., Zhang, F., Riedel, B., Gerke, M., Schwalb, A., and Mäusbacher, R.: Insights into a remote cryosphere: a multi-method approach to assess permafrost occurrence at the Qugaqie basin, western Nyainqêntanglha Range, Tibetan Plateau, The Cryosphere, 15, 149–168, https://doi.org/10.5194/tc-15-149-2021, 2021.

Cao, B., Li, X., Feng, M., and Zheng, D.: Quantifying Overestimated Permafrost Extent Driven by Rock Glacier

445   Inventory, Geophysical Research Letters, 48, 10.1029/2021gl092476, 2021.

Cheng, G., Zhao, L., Li, R., Wu, X., Sheng, Y., Hu, G., Zou, D., Jin, H., Li, X., and Wu, B.: Characteristic, changes and impacts of permafrost on Qinghai-Tibet Plateau (in Chinese), Chinese Science Bulletin, 64, 2783-2795, 10.1360/TB-2019-0191, 2019.

Cicoira, A., Marcer, M., Gärtner-Roer, I., Bodin, X., Arenson, L. U., and Vieli, A.: A general theory of rock

450   glacier creep based on in-situ and remote sensing observations, Permafrost and Periglacial Processes, 32, 139–153, https://doi.org/10.1002/ppp.2090, 2021.

Colucci, R. R., Boccali, C., Zebre, M., and Guglielmin, M.: Rock glaciers, protalus ramparts and pronival ramparts in the south-eastern Alps, Geomorphology, 269, 112-121, 10.1016/j.geomorph.2016.06.039, 2016.

Cui, P., Guo, X., Jiang, T., Zhang, G., and Jin, W.: Disaster Effect Induced by Asian Water Tower Change and

455   Mitigation Strategies, Bulletin of the Chinese Academy of Sciences, 34, 1313-1321, 2019.

Du, Y. Y., Yi, J. W.: Data of climatic factors of annual mean temperature in the Xizang (1990-2015), National Tibetan Plateau Data Center [data set], 2019.

Du, Y. Y., Yi, J. W.: Data set of annual rainfall and climate factors in Tibet (1990-2015), National Tibetan Plateau Data Center [data set], 2019.

460   Emmert, A. and Kneisel, C.: Internal structure of two alpine rock glaciers investigated by quasi-3-D electrical resistivity imaging, The Cryosphere, 11, 841–855, https://doi.org/10.5194/tc-11-841-2017, 2017.

French, H. M.: The Periglacial Environments (3rd Ed.), John Wiley & Sons Ltd, Chichester, UK, xviii + 458 pp, 2007.

Giardino, J. R. and Vitek, J. D.: The significance of rock glaciers in the glacial-periglacial landscape continuum, Journal of Quaternry Science, 3, 97-103, https://doi.org/10.1002/jqs.3390030111, 1988.

Gruber, S.: Derivation and analysis of a high-resolution estimate of global permafrost zonation, The Cryosphere, 6, 221-233, 10.5194/tc-6-221-2012, 2012.

Guo Z: Inventorying and spatial distribution of rock glaciers in the Yarlung Zangbo River Basin, Ph.D. thesis, Institute of International Rivers and Eco-Security, Yunnan University, China, 77pp., 2019.

Haeberli, W.: Creep of Mountain Permafrost: Internal Structure and Flow of Alpine Rock Glaciers, Mitteilungen der Versuchan-stalt fur Wasserbau, Hydrologie und Glaziologie (Zürich), 77, 1985.

Haeberli, W., Hallet, B., Arenson, L., Elconin, R., Humlum, O., Kääb, A., Kaufmann, V., Ladanyi, B., Matsuoka, N., Springman, S., and Mühll, D. V.: Permafrost creep and rock glacier dynamics, Permafrost and Periglacial Processes, 17, 189-214, https://doi.org/10.1002/ppp.561, 2006.

Halla, C., Blöthe, J. H., Tapia Baldis, C., Trombotto Liaudat, D., Hilbich, C., Hauck, C., and Schrott, L.: Ice content and interannual water storage changes of an active rock glacier in the dry Andes of Argentina, The Cryosphere, 15, 1187–1213, https://doi.org/10.5194/tc-15-1187-2021, 2021.

Hassan, J., Chen, X., Muhammad, S., and Bazai, N. A.: Rock glacier inventory, permafrost probability distribution modeling and associated hazards in the Hunza River Basin, Western Karakoram, Pakistan, Sci Total Environ, 782, 146833, 10.1016/j.scitotenv.2021.146833, 2021.

Hausmann, H., Krainer, K., Brueckl, E., and Ullrich, C.: Internal structure, ice content and dynamics of Ölgrube and Kaiserberg rock glaciers (Ötztal Alps, Austria) determined from geophysical surveys, Austrian Journal of Earth Sciences, 105, 12-31, 2012.

Humlum, O.: Rock Glacier Appearance Level and Rock Glacier Initiation Line Altitude: A Methodological Approach to the Study of Rock Glaciers, Arctic and alpine research, 20, 160-178, 10.2307/1551495, 1988.

Humlum, O.: The climatic significance of rock glaciers, Permafrost and Periglacial Processes, 9, 375-395, 10.1002/(sici)1099-1530(199810/12)9:4<375::Aid-ppp301>3.0.Co;2-0, 1998.

IBM Corp. IBM SPSS Statistics for Windows, Version 27.0, Armonk, New York, 2020.

Ikeda, A., Matsuoka, N., and Kääb, A.: Fast deformation of perennially frozen debris in a warm rock glacier in the Swiss Alps: An effect of liquid water, Journal of Geophysical Research: Earth Surface, 113, https://doi.org/10.1029/2007JF000859, 2008.

Janke, J., Bellisario, A., and Ferrando, F.: Classification of debris-covered glaciers and rock glaciers in the Andes of central Chile, Geomorphology, 241, 98–121, https://doi.org/10.1016/j.geomorph.2015.03.034, 2015.

Janke, J. and Bolch, T.: Rock Glaciers. Reference Module in Earth Systems and Environmental Sciences, 2021.

Ji, J.Q., Zhong, D. L., Ding, L., Zhang, J.J., and Yang, Y. C.: Genesis and scientific significance of the Yarlung Zangbo Canvon, Earth Science Frontiers, 6, 231-235, 10.3321/j.issn:1005-2321.1999.04.005, 1999.

Jones, D. B., Harrison, S., Anderson, K., and Betts, R. A.: Mountain rock glaciers contain globally significant water stores, Scientific Reports, 8, 2834, 10.1038/s41598-018-21244-w, 2018a.

Jones, D. B., Harrison, S., Anderson, K., Selley, H. L., Wood, J. L., and Betts, R. A.: The distribution and hydrological significance of rock glaciers in the Nepalese Himalaya, Global and Planetary Change, 160, 123-142, 10.1016/j.gloplacha.2017.11.005, 2018b.

Jones, D. B., Harrison, S., Anderson, K., and Whalley, W. B.: Rock glaciers and mountain hydrology: A review, Earth-Science Reviews, 193, 66-90, 10.1016/j.earscirev.2019.04.001, 2019b.

Jones, D. B., Harrison, S., Anderson, K., Shannon, S., and Betts, R. A.: Rock glaciers represent hidden water
505   stores in the Himalaya, Sci Total Environ, 793, 145368, 10.1016/j.scitotenv.2021.145368, 2021.

Kääb, A., Haeberli, W., and Gudmundsson, G. H.: Analysing the creep of mountain permafrost using high
precision aerial photogrammetry: 25 years of monitoring Gruben Rock Glacier, Swiss Alps, Permafrost and
Periglacial Processes, 8, 409-426, 10.1002/(sici)1099-1530(199710/12)8:4<409::Aid-ppp267>3.0.Co;2-c, 1997.

Krainer, K., Bressan, D., Dietre, B., Haas, J. N., Hajdas, I., Lang, K., Mair, V., Nickus, U., Reidl, D., Thies, H.,
510   and Tonidandel, D.: A 10,300-year-old permafrost core from the active rock glacier Lazaun, southern Ötztal
Alps   (South   Tyrol,   northern   Italy),   Quaternary   Research,   83,   324–335,
https://doi.org/10.1016/j.yqres.2014.12.005, 2015.

Krainer, K., and Mostler, W.: Reichenkar rock glacier: a glacier derived debris-ice system in the western Stubai
Alps, Austria, Permafrost and Periglacial Processes, v. 11, no. 3, p. 267-275, 2000.

515   Krainer, K. and Ribis, M.: A rock glacier inventory of the Tyrolean alps (Austria), Austrian Journal of Earth
Sciences, 105, 32–47, 2012.

Korup, O. and Montgomery, D. R.: Tibetan plateau river incision inhibited by glacial stabilization of the
Tsangpo Gorge, Nature, 455, 786-U784, 10.1038/nature07322, 2008.

Lilleøren, K.S. and Etzelmüller, B.: A regional inventory of rock glaciers and ice‐cored moraines in Norway,
520   Geografiska   Annaler: Series   A,   Physical   Geography,   93,   175-191,
https://doi.org/10.1111/j.1468-0459.2011.00430.x, 2011.

Linsbauer, A., Paul, F., Hoelzle, M., Frey, H., and Haeberli, W.: The Swiss Alps Without Glaciers - A
GIS-based Modelling Approach for Reconstruction of Glacier Beds, https://doi.org/10.5167/uzh-27834, 2009.

Liu, G. N., Xiong, H. G., Cui, Z. J., and Song, C. Q.: The morphological features and environmental condition
525   of rock glaciers in Tianshan mountains, Scientia Geographica Sinica, 15, 226-233, 297, 1995.

Liu, S., Guo, W., Xu, J.: The second glacier inventory dataset of China (version 1.0) (2006-2011). National
Tibetan Plateau Data Center [data set], 10.3972/glacier.001. 2013.db, 2012.

Long, D., Li, X. Y., Li, X. D., Han, P. F., Zhao, F. Y., Hong, Z. K., Wang, Y. M., and Tian, F. Q.: Remote
sensing retrieval of water storage changes and underlying climatic mechanisms over the Tibetan Plateau during
530   the past two decades, Advances in Water Science, 33, 375-389, 10.14042/j.cnki.32.1309.2022.03.003, 2022.

Magori, B., Urdea, P., Onaca, A., and Ardelean, F.: Distribution and characteristics of rock glaciers in the
Balkan   Peninsula,   Geografiska   Annaler: Series   A,   Physical   Geography,   102,   354-375,
10.1080/04353676.2020.1809905, 2020.

Mathys, T., Hilbich, C., Arenson, L. U., Wainstein, P. A., and Hauck, C.: Towards accurate quantification of ice
535   content in permafrost of the Central Andes – Part 2: An upscaling strategy of geophysical measurements to the
catchment scale at two study sites, The Cryosphere, 16, 2595–2615, https://doi.org/10.5194/tc-16-2595-2022,
2022.

Millar, C. I. and Westfall, R. D.: Rock glaciers and related periglacial landforms in the Sierra Nevada, CA, USA;
inventory,   distribution   and   climatic   relationships,   Quaternary   International,   188,   90-104,
540   10.1016/j.quaint.2007.06.004, 2008.

Millar, C. I., Westfall, R. D., and Delany, D. L.: Thermal and hydrologic attributes of rock glaciers and
periglacial talus landforms: Sierra Nevada, California, USA, Quaternary International, 310, 169-180,
10.1016/j.quaint.2012.07.019, 2013.

Müller, J., Vieli, A., and Gärtner-Roer, I.: Rock glaciers on the run – understanding rock glacier landform evolution and recent changes from numerical flow modeling, The Cryosphere, 10, 2865–2886, https://doi.org/10.5194/tc-10-2865-2016, 2016.

Ni, J., Wu, T., Zhu, X., Hu, G., Zou, D., Wu, X., Li, R., Xie, C., Qiao, Y., Pang, Q., Hao, J., and Yang, C.: Simulation of the Present and Future Projection of Permafrost on the Qinghai-Tibet Plateau with Statistical and Machine Learning Models, Journal of Geophysical Research: Atmospheres, 126, e2020JD033402, https://doi.org/10.1029/2020JD033402, 2021.

Nyenhuis, M., Hoelzle, M., and Dikau, R.: Rock glacier mapping and permafrost distribution modelling in the Turtmanntal, Valais, Switzerland, Zeitschrift fur Geomorphologie, 49, 275–292, 2005.

Pan, G. T., Wang, L. Q., Zhang, W. P., Wang, B. D.: Tectonic Map and Specification of Qinghai Tibet Plateau and Its Adjacent Areas (1: 1 500 000), Geology Press, Beijing, 208pp, 2013.

Pandey, P.: Inventory of rock glaciers in Himachal Himalaya, India using high-resolution Google Earth imagery, Geomorphology, 340, 103-115, 10.1016/j.geomorph.2019.05.001, 2019.

Paterson, W. S. B.: The Physics of Glaciers, Butterworth-Heinemann, Oxford, 480pp, 1994.

Pfeffer, W. T., Arendt, A. A., Bliss, A., Bolch, T., Cogley, J. G., Gardner, A. S., Hagen, J. O., Hock, R., Kaser, G., Kienholz, C., Miles, E. S., Moholdt, G., Mölg, N., Paul, F., Radic, V., Rastner, P., Raup, B. H., Rich, J., and Sharp, M. J.: The Randolph Glacier inventory: a globally complete inventory of glaciers, Journal of Glaciology, 60, 537-552, 2014.

Ran, Y., Li, X., Cheng, G., Nan, Z., Che, J., Sheng, Y., Wu, Q., Jin, H., Luo, D., Tang, Z., and Wu, X.: Mapping the permafrost stability on the Tibetan Plateau for 2005–2015, Science China Earth Sciences, 64, 62-79, 10.1007/s11430-020-9685-3, 2020.

Ran, Z. and Liu, G.: Rock glaciers in Daxue Shan, south-eastern Tibetan Plateau: an inventory, their distribution, and their environmental controls, The Cryosphere, 12, 2327-2340, 10.5194/tc-12-2327-2018, 2018.

Rangecroft, S., Harrison, S., and Anderson, K.: Rock glaciers as water stores in the Bolivian Andes: an assessment of their hydrological importance, Arctic Antarctic and Alpine Research, 47, 89-98, 10.1657/aaar0014-029, 2015.

Rangecroft, S., Suggitt, A. J., Anderson, K., and Harrison, S.: Future climate warming and changes to mountain permafrost in the Bolivian Andes, Clim Change, 137, 231-243, 10.1007/s10584-016-1655-8, 2016.

Reinosch, E., Gerke, M., Riedel, B., Schwalb, A., Ye, Q., and Buckel, J.: Rock glacier inventory of the western Nyainqêntanglha Range, Tibetan Plateau, supported by InSAR time series and automated classification, Permafrost and Periglacial Processes, 32, 657-672, 10.1002/ppp.2117, 2021.

RGIK. Towards standard guidelines for inventorying rock glaciers: baseline concepts (version 4.2.2). IPA Action Group Rock glacier inventories and kinematics, 13 pp, 2022a.

RGIK. Towards standard guidelines for inventorying rock glaciers: practical concepts (version 2.0). IPA Action Group Rock glacier inventories and kinematics, 10 pp. 2022b.

Sattler, K., Anderson, B., Mackintosh, A., Norton, K., and de Róiste, M.: Estimating Permafrost Distribution in the Maritime Southern Alps, New Zealand, Based on Climatic Conditions at Rock Glacier Sites, Frontiers in Earth Science, 4, 10.3389/feart.2016.00004, 2016.

Schaffer, N., MacDonell, S., Réveillet, M., Yáñez, E., and Valois, R.: Rock glaciers as a water resource in a changing climate in the semiarid Chilean Andes, Regional Environmental Change, 19, 1263-1279,

10.1007/s10113-018-01459-3, 2019.

585   Schmid, M. O., Baral, P., Gruber, S., Shahi, S., Shrestha, T., Stumm, D., and Wester, P.: Assessment of permafrost distribution maps in the Hindu Kush Himalayan region using rock glaciers mapped in Google Earth, Cryosphere, 9, 2089-2099, 10.5194/tc-9-2089-2015, 2015.

Schrott, L.: Some geomorphological-hydrological aspects of rock glaciers in the Andes (San Juan, Argentina), Zeitschrift fur Geomorphologie, Supplementband, 104, 161–173, 1996.

590   Schoeneich, P., Bodin, X., Echelard, T., Kaufmann, V., Kellerer-Pirklbauer, A., Krysiecki, J.-M., and Lieb, G. K.: Velocity Changes of Rock Glaciers and Induced Hazards, in: Engineering Geology for Society and Territory - Volume 1, Cham, 223–227, 2015.

Scotti, R., Brardinoni, F., Alberti, S., Frattini, P., and Crosta, G. B.: A regional inventory of rock glaciers and protalus ramparts in the central Italian Alps, Geomorphology, 186, 136-149, 10.1016/j.geomorph.2012.12.028, 595   2013.

Selley, H., Harrison, S., Glasser, N., Wündrich, O., Colson, D., and Hubbard, A.: Rock glaciers in central Patagonia, Geografiska Annaler: Series A, Physical Geography, 101, 1-15, 10.1080/04353676.2018.1525683, 2018.

Wagner, T., Kainz, S., Helfricht, K., Fischer, A., Avian, M., Krainer, K., and Winkler, G.: Assessment of liquid 600   and solid water storage in rock glaciers versus glacier ice in the Austrian Alps, SCIENCE OF THE TOTAL ENVIRONMENT, 800, https://doi.org/10.1016/j.scitotenv.2021.149593, 2021.

Wahrhaftig, C. and Cox, A.: Rock glaciers in the Alaska Range, GSA Bulletin, 70, 383-436, 10.1130/0016-7606(1959)70[383:Rgitar]2.0.Co;2, 1959.

Xiang, S. Y.: 1:3 million Quaternary geological and geomorphological map of the Tibetan Plateau and its 605   surrounding areas, China University of Geosciences Press, Wuhan, 104pp, 2013.

Yao, T., Wu, G., Xu, B., Wang, W., Gao, J., and An, B.: Asian Water Tower Change and Its Impacts, Bulletin of the Chinese Academy of Sciences, 34, 1203-1209, 2019.

Yao, T., Bolch, T., Chen, D., Gao, J., Immerzeel, W., Piao, S., Su, F., Thompson, L., Wada, Y., Wang, L., Wang, T., Wu, G., Xu, B., Yang, W., Zhang, G., and Zhao, P.: The imbalance of the Asian water tower, Nature 610   Reviews Earth & Environment, 3, 618–632, https://doi.org/10.1038/s43017-022-00299-4, 2022.

Yu, X., Ji, J., Gong, J., Sun, D., Qing, J., Wang, L., Zhong, D., and Zhang, Z.: Evidence of rapid erosion driven by climate in the Yarlung Zangbo (Tsangpo) Great Canyon, the eastern Himalayan syntaxis, Chinese Science Bulletin, 56, 1123-1130, 10.1007/s11434-011-4419-x, 2011.

Zhang, Q., Jia, N., Xu, H., Yi, C., Wang, N., and Zhang, L.: Rock glaciers in the Gangdise Mountains, southern 615   Tibetan Plateau: Morphology and controlling factors, CATENA, 218, 106561, https://doi.org/10.1016/j.catena.2022.106561, 2022.

Zheng J, Yin Y, Li B. A New Scheme for Climate Regionalization in China, ACTA GEOGRAPHICA SINICA, 65, 3-12, 10.11821/xb201001002, 2010.

Zhou Y, Guo D, Qiu G, Cheng G, Li S. Geocryology In China, Science Press, Beijing, 450pp, 2000.

620